Postmodification via Thiol-click Chemistry Yields Hydrophilic Trityl-nitroxide Biradicals for Biomolecular High-Field Dynamic Nuclear Polarization

Weixiang Zhai,[1][‡] Alessandra Lucini Paioni,[2][‡] Xinyi Cai, [1] Siddarth Narasimhan, [2] João Medeiros-Silva, [2]Wenxiao Zhang, [1] Antal Rockenbauer, [3] Markus Weingarth, [2] Yuguang Song, [1] Marc Baldus[2] and Yangping Liu[1]**

[1]Tianjin Key Laboratory on Technologies Enabling Development of Clinical Therapeutics and Diagnostics, School of Pharmacy, Tianjin Medical University, Tianjin 300070, P. R. China.

[2]NMR Spectroscopy, Bijvoet Centre for Biomolecular Research, Utrecht University, 3584 CH Utrecht, The Netherlands.

[3]Institute of Materials and Environmental Chemistry, Hungarian Academy of Sciences and, Department of Physics, Budapest University of Technology and Economics, Budafokiut 8, 1111 Budapest, Hungary.

ABSTRACT

Dynamic nuclear polarization (DNP) is a powerful method to enhance nuclear magnetic resonance (NMR) signal intensities, enabling unprecedented applications in life and material science. An ultimate goal is to expand the use of DNP-enhanced solid-state NMR to ultra-high magnetic fields where optimal spectral resolution and sensitivity are integrated. Trityl-nitroxide (TN) biradicals have attracted significant interest in high-field DNP, but their application to complex (bio)molecules has so far been limited. Here we report a novel postmodification strategy for synthesis of hydrophilic TN biradicals in order to improve their biomolecular applications. Initially, three TN biradicals (referred as to NATriPols 1-3) with amino-acid linkers were synthesized. EPR studies showed that the α-position of the amino-acid linkers is an ideal modification site for these biradicals since their electron-electron magnetic interactions are marginally affected by the substituents at this position. Based on this finding, we synthesized NATriPol-4 with pyridine disulfide appended at the α-position. Postmodification of NATriPol-4 via thiol-click chemistry resulted in various TN biradicals including hydrophilic NATriPol-5 in a quantitative manner. Interestingly, DNP enhancements at 18.8 T of NATriPols for $^{13}C,^{15}N$-proline in a glycerol/water matrix are inversely correlated with their hydrophobicity. Importantly, applications of hydrophilic NATriPol-5 and NATriPol-3 to biomolecules including a globular soluble protein and a membrane targeting peptide reveal significantly improved performance compared to TEMTriPol-1 and AMUPol. Our work provides an efficient approach for one-step synthesis of new polarizing agents with tunable physicochemical properties, thus expediting optimization of new biradicals for biomolecular applications at ultra-high magnetic fields.

1
2
3
4
5
6
7
8
9
10
11
12
13
14
15
16
17
18
19
20
21
22
23
24
25
26
27
28
29
30
31
32
33
34
35
36
37
38
39
40
41
42
43
44
45
46
47
48
49
50
51
52
53
54
55
56
57
58
59
60

Introduction

Dynamic nuclear polarization (DNP) has evolved into a well-established and powerful technique to enhance the sensitivity of nuclear magnetic resonance (NMR) spectroscopy in the liquid[1-2] and solid state[3-5] by microwave-driven transfer of polarization from unpaired electrons (i.e., polarizing agents) to nuclei. Signal enhancements by several orders of magnitude when using DNP create entirely new application areas of solid-state NMR (ssNMR) in structural biology[6-11] and material science.[4, 12-16] In parallel, recent innovations in DNP instrumentation (including microwave sources and low-temperature NMR/DNP probeheads),[17-18] have allowed to extend DNP-enhanced ssNMR to ultra-high magnetic fields (up to 21.1 T)[19-23] and the potential to increase spectral resolution under such conditions has already been demonstrated.[20, 24]

At high field and low temperatures (typically 100 K), the cross effect (CE) has so far proven to be the most efficient mechanism, which requires a coupled three-spin system consisting of two electrons and one nucleus.[3-4, 25] To fulfill the CE condition, biradicals are routinely used as polarizing agents. In the past decade, much effort has been devoted to improve nitroxide-based biradical polarizing agents by optimizing g tensor orientations, rigidity of the linker and electron spin relaxation times.[26-31] These efforts have led to the development of efficient nitroxide biradicals such as AMUPol[28] and TEKPol[29] that possess DNP enhancement factors ($\varepsilon_{on/off}$) of up to ~ 250 at moderate magnetic fields (e.g., 9.4 T) under magic-angle spinning (MAS) conditions. In parallel, theoretical approaches and numerical studies have been employed to understand the factors determining the CE polarization efficiency and to guide the design of new polarizing agents.[32-36]

Ideally, MAS-DNP experiments are carried out at high magnetic fields where the spectral resolution is maximized together with further improved sensitivity. Although nitroxide biradicals exhibit satisfying performance below 10 T, their DNP enhancements rapidly decrease as the magnetic field is increased. For instance, the ^{1}H signal enhancements drop from 250 at 5 T to approximately 30 at 18.8 T for AMUPol (10 mM) in the conventional "DNP juice" (d_8-glycerol/D_2O/H_2O, 60/30/10, V/V/V).[37] These values could be further attenuated after considering nuclear depolarization and quenching effects induced by the paramagnetic polarizing agents.[32, 38-40] The unfavourable correlation of the DNP enhancements of the nitroxide biradicals with the external field is partially due to the linear broadening of their EPR linewidths with the field and the MAS-dependence of the underlying dipolar electron-electron interactions (D).[33, 41] Hence, very recently, efforts have been devoted towards the development of novel dinitroxide biradicals that show excellent DNP performances with the $\varepsilon_{on/off}$ values of up to 90 for the TinyPols series at high fields and high spinning frequencies.[22] However, these enhancement values were obtained using 1.3 mm MAS rotors where the microwave field distribution is more favorable than in 3.2 mm rotors used in our current study. Moreover, these dinitroxides still exhibit the unfavorable field dependence albeit attenuated when compared to AMUPol.

In collaboration with the Griffin group,[37] we found that trityl-nitroxide (TN) mixed biradicals (also referred to as TEMTriPols), initially developed as electron paramagnetic resonance (EPR) probes for the redox status,[42-43] exhibit remarkable DNP properties. In contrast to nitroxide biradicals, the DNP enhancements of TEMTriPols exhibit favorable magnetic-field dependence and the optimal value is displaced towards higher magnetic fields.[37] For example, TEMTriPol-1 shows DNP enhancement factors for ^{13}C-labeled urea of 50, 87 and 65 at 5.0, 14.1 and 18.8T, respectively, without a significant depolarization effect at the chosen MAS settings.[44]

Thus, the signal enhancement obtained using TEMTriPol-1 in hydrophilic environments at 18.8 T still represents the highest value among the currently available biradicals using 3.2 mm MAS rotors. The distinct DNP properties of TEMTriPols can be explained by their unique physicochemical properties including (i) the ideal EPR frequency separation between the nitroxide g_{yy} component and the almost isotropic g value of trityl radical; (ii) their favourable relaxation times, which allow simultaneous microwave saturation and polarization turnover; (iii) moderate electron-electron exchange interactions (J) which are beneficial for their DNP performance at high fields.[41, 45]

Likewise, other hybrid biradicals (e.g., BDPA-nitroxide[22, 46-47] and PTM-nitroxide biradicals[48], and asymmetric nitroxide biradicals[34]) were developed for high-field DNP or fast dissolution DNP, although most of them are not compatible with biomolecular studies due to their high hydrophobicity. In these studies, the importance of the total size of dipolar and exchange interactions for high-field DNP properties of biradicals was also highlighted. Recently, we have confirmed the influence of the exchange interaction on the DNP enhancement using chiral TN biradicals that exhibit almost identical dipolar interactions but completely different exchange interactions.[49] Certainly, optimal dipolar/exchange interactions for a biradical may exist. They should be large enough to maintain the polarization difference between two spins by efficient polarization transfer and, at the same time, sufficiently small to preserve the frequency matching required for DNP.[49]Moreover, a recent study suggested that the relative intensity of exchange to dipolar interactions (J/D) is a crucial factor for CE-DNP.[50] Recent theoretical studies predicted that TEMTriPol-1 has approached the optimal dipolar/exchange interactions.[34, 44] Therefore, further optimization of other physicochemical properties of TEMTriPol-1 while maintaining its dipolar/exchange interactions may be an effective method to design new

powerful polarizing agents. High hydrophilicity is critical for biomolecular applications[51] which mostly involve the use of AMUPol and TOTAPol[52] because of their good water solubility. Accordingly, there is a great need to develop new TN biradicals which exhibit nearly identical dipolar/exchange interactions as TEMTriPol-1 but with improved hydrophilicity.

In this work, we report a novel postmodification approach to synthesize hydrophilic TN biradicals via thiol-click chemistry. Firstly, based on the molecular structure of TEMTriPol-1, we synthesized three TN biradicals (NATriPol 1-3, Chart 1) in which α-amino acids such as L-alanine, L-phenylalanine and L-aspartic acid were used as linkers. EPR experiments confirm that these biradicals exhibit very similar electron-electron dipolar/exchange interactions. Based on these findings, the pyridine disulfide-appended NATriPol-4 was further synthesized from which NATriPol-5 was obtained through a "click" reaction with glutathione in a quantitative manner. We measured the DNP performance of these NATriPols using standard DNP preparations at 18.8 T and investigated the relationship between DNP enhancement and hydrophobicity. Using the hydrophilic NATriPol-3 and -5 at 10 mM concentration, we observed strong absolute signal gains (ε_{abs}) of up to 60 for [^{13}C-,^{15}N]-proline, achieving a new maximum of the DNP enhancement at 18.8 T using 3.2 mm MAS rotor in hydrophilic environments. Furthermore, experiments employing [^{13}C-,^{15}N]-algal amino acid mixtures, [^{13}C-,^{15}N]-ubiquitin and a membrane-associated peptide confirm the excellent DNP performance of NATriPol-3 and -5 and reveal their potential for biomolecular applications.

BIRADICAL	R
TEMTriPol-1	H
NATriPol-1	CH_3
NATriPol-2	CH_2Ph
NATriPol-3	CH_2COOH
NATriPol-4	CH_2SSPy
NATriPol-5	CH_2SSG

Chart 1. Molecular structure of NATriPols and TEMTriPol-1. Note: SPy, 2-pyridinylthio; SG, glutathionyl.

Methods

General Information

All reactions were carried out under argon atmosphere. Dichloromethane (CH_2Cl_2) was redistilled with CaH_2 and dimethylformamide (DMF) were passed through a column of molecular sieves. Boc-L-alanine, Boc-L-phenylalanine, 4-tert-butyl-N-Fmoc-L- aspartate, N-Fmoc-S-trityl-L-cysteine, 1-hydroxybenzotriazole (HOBt), (benzotriazol-1-yloxy) tris(dimethylamino) phosphoniumhexafluoro-phosphate (BOP), N,N-diisopropylethyl-amine (DIPEA), 2,2,6,6-tetramethyl-4-amino-piperidine-1-oxyl free radical, trifluoroacetic acid (TFA), triethylsilane, piperidine, 2,2'-dithiodipyridine, cysteine (Cys), 4-mercaptobenzoic acid (4-MBA) and glutathione (GSH) were purchased and used without further purification. The [$^{13}C,^{15}N$] Algal amino-acid mixture was purchased from Cortecnet. CT-03 was prepared according to the previously reported method.[53] Thin layer chromatography analysis was performed on glass 0.25 mm silica gel plates which were visualized by exposure to UV light. Flash column chromatography was employed using silica gel with 200-300 mesh. High-

resolution mass spectrometry was carried out employing electrospray ionization methods (ESI) for the end products and LTQ Orbitrap discovery (ESI, Thermofisher scientific) for the reaction intermediates. EPR measurements were carried out on Bruker EMX-plus X-band spectrometer. Analytical HPLC was done on an Agilent 1100 instrument equipped with a G1315B DAD detector and G1311A pump, and data are shown in Fig. S1. Semipreparative HPLC was carried out on SSI 1500 equipped with a UV/Vis detector and versa-pump. The UV-Vis absorption spectra were recorded at room temperature on a U-3900 UV-Vis spectrophotometer equipped with a 1 cm quartz cell.

Synthesis

NAC-1, NAC-2, NAC-3 and NAC-4

BOP (938 mg, 2.12 mmol) was added to a solution containing Fmoc-L-aspartic acid beta-tert-butyl ester (435 mg, 1.06 mmol), HOBt (430 mg, 3.18 mmol) and DIPEA (0.9 mL, 5.30 mmol) in CH_2Cl_2 (5 mL). The resulting solution was stirred at ambient temperature for 0.5 h. Then, a solution of 2,2,6,6-tetramethyl-4-amino-piperidine-1-oxyl free radical (218 mg, 1.27 mmol) in CH_2Cl_2 (2 mL) was added and the reaction mixture was stirred at 25 °C for another 3 h. CH_2Cl_2 (30 mL) was added and the organic layer washed successively with 6% citric acid (30 mL), saturated solution of $NaHCO_3$ (30 mL) and brine (30 mL). The organic layer was dried over anhydrous sodium sulfate, filtered and concentrated in vacuo. The crude residue was purified by flash column chromatography on silica gel using EtOAc/petroleum ether (1:2) as an eluent to give the precursor of NAC-3 (521 mg, 87% yield) as a red solid. The precursor was directly used in the next step without further characterization. A similar procedure was utilized for the synthesis of the precursors of NAC-1, NAC-2 and NAC-4, using Boc-L-alanine, Boc-L-

phenylalanine and N-Fmoc-S-trityl-L- cysteine, respectively, as the starting materials instead of Fmoc-L-Aspartic acid beta-tert-butyl ester.

Then the precursor of NAC-1 (100 mg, 0.29 mmol) in CH_2Cl_2 (1 mL) was treated with trifluoroacetic acid (TFA, 1 mL) and the resulting solution was stirred at 25 ºC for 4 h. After removing the solvents under vacuo, the residue was redissolved in EtOAc (30 mL), and washed with saturated solution of $NaHCO_3$ (30 mL) and brine (30 mL). The organic layer was dried over anhydrous sodium sulfate, filtered and concentrated in vacuo to afford NAC-1 (62 mg, 89 %) as a red solid. BOC-NAC-1, HRMS (ESI, m/z): calcd for $C_{17}H_{32}N_3O_4^{•+}$ ($[M+Na]^+$), 365.2285; found, 365.2285. Using a similar procedure, NAC-2 (66 mg, 87 %) was obtained from the corresponding precursor. BOC-NAC-2, HRMS (ESI, m/z): calcd for $C_{23}H_{36}N_3O_4^{•+}$ ($[M+Na]^+$), 441.2598; found, 441.2599.

On the other hand, the precursor of NAC-3 (283 mg, 0.50 mmol) or NAC-4 (200 mg, 0.27 mmol) in CH_2Cl_2 (4 mL) was treated with piperidine (1 mL). The resulting solution was stirred at 25 ºC for 4 h. Then, CH_2Cl_2 (30 mL) was added and the organic layer was washed successively with 6% citric acid (30 mL), saturated solution of $NaHCO_3$ (30 mL) and brine (30 mL). The organic layer was dried over anhydrous sodium sulfate, filtered and concentrated in vacuo. The crude residue was purified by flash column chromatography on silica gel using 5% MeOH in CH_2Cl_2 as an eluent to give NAC-3 (155 mg, 91%) or NAC-4 (123 mg, 88%) as red solid. NAC-3, HRMS (ESI, m/z): calcd for $C_{17}H_{32}N_3O_4^{•+}$($[M+H]^+$), 343.2466; found, 343.2471. NAC-4, HRMS (ESI, m/z): calcd for $C_{31}H_{38}N_3O_2S^{•+}$ ($[2M+H]^+$), 1033.5442; found, 1033.5447.

NATriPol-1 and NATriPol-2

BOP (18 mg, 0.04 mmol) was added to a solution containing CT-03 (40 mg, 0.04 mmol), HOBt (16 mg, 0.12 mmol) and DIPEA (70 μL, 0.40 mmol) in DMF (3 mL). The resulting

solution was stirred at 25 ºC for 0.5 h and then mixed with NAC-1 (39 mg, 0.16 mmol) in DMF

(2 mL). After stirring at 25 °C for 18 h, the reaction mixture was poured into EtOAc (30 mL) and

1 M HCl (30 mL). The organic layer was separated, washed with brine (30 mL), dried over

anhydrous sodium sulfate, filtered and concentrated in vacuo. The resulting residue was

dissolved in phosphate buffer (0.2 M, pH 7.4) and purified by column chromatography on

reversed-phase C18 using water followed by 0-40% MeOH in H_2O as eluents to give NATriPol-

1 (26 mg, 53%). HRMS (ESI, m/z): calcd for $C_{52}H_{61}N_3O_7S_{12}^{\bullet-}$ ([M-H]$^-$), 1222.1080; found,

1222.1071. HPLC: 13.68 min.

Similarly, using NAC-2 as a starting material, NATriPol-2 was obtained as a green solid (30

mg, 58%). HRMS (ESI, m/z): calcd for $C_{58}H_{65}N_3O_7S_{12}^{\bullet-}$ ([M-H]$^-$), 1298.1393; found,

1298.1378. HPLC: 14.81 min.

NATriPol-3

Using a procedure similar to the synthesis of NATriPol-1, PAP-1 (55 mg, 0.04 mmol) was

obtained from NAC-3 (27 mg, 0.08 mmol). Then, PAP-1 was dissolved in CH_2Cl_2 (2 mL) and

TFA (2 mL). The resulting solution was stirred at 25 ºC for 4 h and the solvents were removed

under vacuo. The resulting residue was dissolved in phosphate buffer (0.2 M, pH 7.4), and

purified by column chromatography on reversed-phase C18 using water followed by 0-40%

MeOH in H_2O as eluents to give NATriPol-3 (25 mg, 49%). HRMS (ESI, m/z): calcd for

$C_{53}H_{61}N_3O_9S_{12}^{\bullet-}$ ([M-H]-), 1266.0978; found, 1266.0997. HPLC: 11.29 min.

NATriPol-4

Using a procedure similar to the synthesis of NATriPol-1, PAP-2 (64 mg, 0.04 mmol) was

obtained from NAC-4 (41 mg, 0.08 mmol). Then, PAP-2 in DMF (2 mL) was treated with TFA

(2 mL) and triethylsilane (6 μL, 1 eq). The reaction mixture was stirred at 25 ºC for 18 h and

then dried under vacuo. The resulting residue was redissolved in MeOH and 2,2'-dithiodipyridine was added. After stirring at 25 ºC for 2 h, the reaction mixture was dried under vacuo redissolved in phosphate buffer (0.2 M, pH 7.4), and then purified by column chromatography on reversed-phase C18 using water followed by 0-40% MeOH in H_2O as eluents to give NATriPol-4 (25 mg, 45%). HRMS (ESI, m/z): calcd for $C_{57}H_{64}N_4O_7S_{14}^{\bullet\bullet-}$ ([M-H]⁻), 1365.0943; found, 1365.0768. HPLC: 14.92 min.

NATriPol-5

The click reaction of NATriPol-4 with GSH (3 equiv.) was carried out in water to afford NATriPol-5 in a quantitative manner. NATriPol-5, HRMS (ESI, m/z): calcd for $C_{62}H_{76}N_6O_{13}S_{14}^{\bullet\bullet+}$ ([M+H]⁺), 1561.1638; found, 1561.1375. HPLC: 11.22 min.

Measurement of Water Solubility

Excess of biradical (carboxylate sodium form) was added as a solid to water. The resulting suspension was centrifuged and the supernatant fraction was separated. Then, after appropriate dilution with water, the concentration of the supernatant (i.e., the water solubility of the biradical) was estimated by UV-Vis spectroscopy according to the pre-determined molar absorption coefficient (16.8 mM⁻¹ cm⁻¹) at 464 nm, assuming that this type of biradicals exhibit the same molar absorption coefficients.

Determination of LogP

The aqueous solution of the biradical (100 μL, 200 μM) was mixed with octanol (100 μL) and the resulting solution was gently shaken for 24 h. Then, the aqueous fraction was separated and the concentration of the biradical in this fraction was determined by EPR double integration. Accordingly, the concentration of the biradical in the octanol layer was calculated. Finally, the

octanol-water partition coefficient (LogP) of the biradical was estimated according to its concentrations in the two fractions.

EPR Measurement

EPR spectra were recorded in phosphate buffer (20 mM, pH 7.4) at room temperature or in glycerol/water (v/v, 60/40) at ~ 220K on a Bruker EMX-plus X-band spectrometer. General instrumental settings were as follows: modulation frequency, 100 kHz; microwave power, 10 mW; modulation amplitude, 1 G (room temperature) and 2 G (low temperature). Measurements were performed in 50 μL capillary tubes.

ESR Simulation:

The room- and low-temperature EPR spectra were simulated by ROKI/EPR program[43] and ROKI/DNP program[49], respectively, which were developed by professor Rockenbauer[54]. ROKI/EPR program could calculate a reliable exchange interaction of TN biradicals. As for the ROKI/DNP program, magnetic resonance parameters including the principal values of the two g- and hyperfine tensors, the Euler angles between the principal directions of tensors, the polar angles of linker, exchange and dipolar interactions can be optimized to achieve the best fit of the experimental spectra. The exchange, dipolar and hyperfine couplings given in Gauss units can be converted to cm^{-1} by multiplying with $4.6686 \times 10^{-5} \times g$, where g is the respective Zeeman factor.

Solution-State NMR Experiments

The samples for the solution-state NMR titration experiments were prepared by dissolving 1mg of lyophilized [^{13}C,^{15}N] ubiquitin in 90/10 H_2O/D_2O solvent, for a final concentration of 0.1mM. Increasing amounts of biradical were then subsequently added to the sample, for final radical concentrations of 0, 0.01 and 0.1mM.

^{15}N-^{1}H HSQC spectra[55] were acquired at 298 K with a triple channel (^{1}H, ^{13}C, ^{15}N) cryogenically cooled-probe, at a static magnetic field of 14 T, corresponding to a proton frequency of 600 MHz with 16 scans with a delay of 1s. Acquisition times were 66 ms and 26 for the ^{1}H and ^{15}N dimensions, respectively. The spectra were processed using a 0.5π sine squared window function in both dimensions.

DNP-ssNMR spectroscopy of NATriPols 1-5

DNP experiments were performed on frozen solutions of 5 mM, 10 mM or 15 mM biradical in d8-glycerol:D_2O:H_2O 60:30:10 v:v:v with 0.25 M U-[13]C-^{15}N proline. Samples were packed into 3.2 mm sapphire rotors with a sample volume of 25 μL. DNP experiments at 800 MHz were performed on a Bruker BioSpin 527 GHz solid-state NMR DNP spectrometer.[20] This spectrometer is equipped with a Bruker 800 WB/RS Plus magnet with a sweep coil, an Avance III NMR console, and a low-temperature 3.2 mm double-resonance DNP MAS NMR probehead. A gyrotron microwave source emits microwaves at a frequency of 527.043 GHz. The nuclear polarization was measured through the spectrum of [13]C-^{15}N proline, which is observed via [1]H-^{13}C cross-polarization (CP) experiments. A CP spin-locking field of 48 kHz was applied on ^{13}C, while a ramped (80-100%) power was employed during a 50 kHz spin-locking field on [1]H. The contact time was set to 2 ms. During acquisition, SPINAL-64[56] decoupling was applied at 83 kHz and a delay of $1.26*T_B$ was employed for optimal sensitivity. Each spectrum was acquired with a 4-step phase cycle and repeated three times to confirm stability and reproducibility. The MAS frequency was set to 8 kHz and the sample temperature was kept at 103 K. The time constant T_B, which describes the buildup of ^{1}H polarization, was measured via a ^{1}H saturation recovery experiment and determined indirectly by detecting the ^{13}C CP signal. The polarization

build up curves were fitted with monoexponential curves and the largest error of the fit was found to be ±5% in the microwaves- off case.

To find the optimal CE DNP enhancement for each radical, the magnetic field was swept and at each field position the nuclear polarization was measured via the cross-polarization experiment as described above.

To perform the DNP experiments on the labeled ubiquitin, 1mg of lyophilized [^{13}C,^{15}N] ubiquitin was dissolved in d8-glycerol:D_2O:H_2O 60:30:10 v:v:v, for a final protein concentration of 4mM.In the same way, 1mg of the^{13}C- ^{15}N- enriched (≥98%) algal amino acid mixture (Cortecnet, CCN070P1) was dissolved in 30ul of standard DNP juice (d8-glycerol:D_2O:H_2O 60:30:10 v:v:v).

For the 2D PDSD experiments, a mixing time of 30 ms and a ^{1}H-^{13}C CP contact time of 0.7 ms were used. A cumulative number of scans of 32 were applied and acquisition times were set to 17 ms and 10 ms for the direct and indirect dimensions, respectively. The experiments were recorded at a MAS rate of 8 kHz, using a 84 kHz SPINAL-64 proton decoupling and a recycle delay of 2 s. The 2D spectra were processed using a 0.5 π shifted sine squared window function on both dimensions (Bruker software Topspin 4.0).
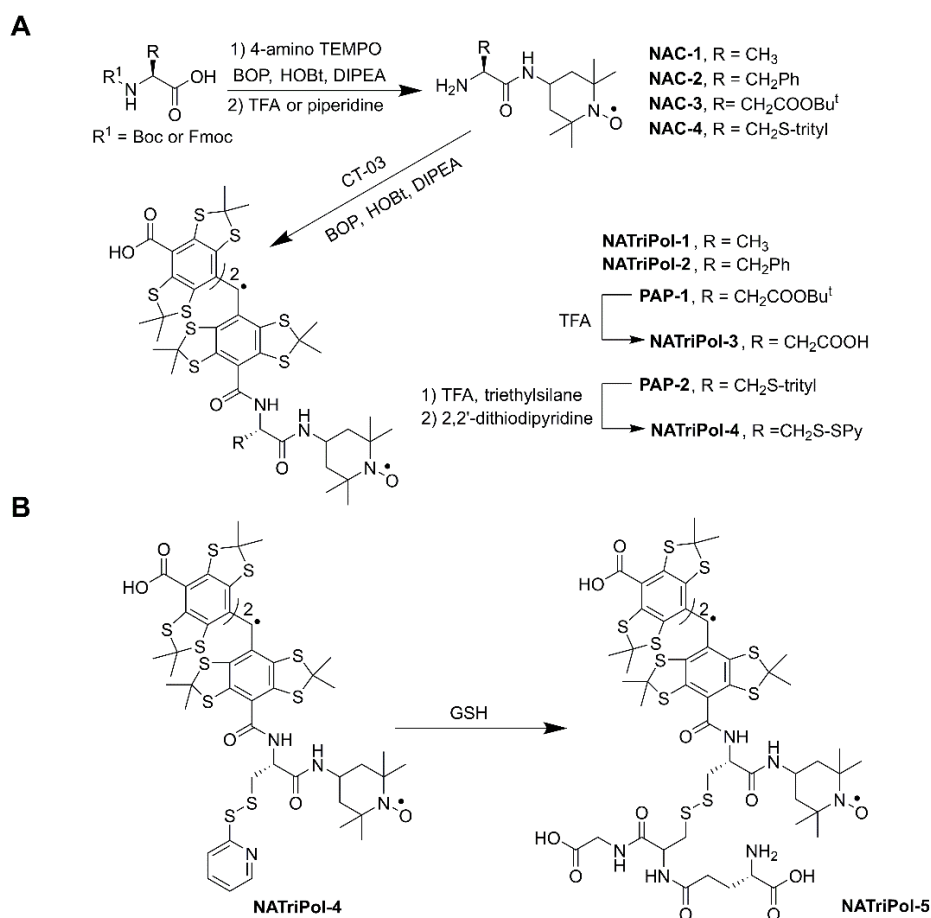
Results and Discussion

Synthesis of NATriPols 1-3

We synthesized amino acid-linked TN biradicals (in the following referred to as NATriPols) from the protected L-amino acids using our previous method with some modifications.[43] 4-Amino-TEMPO (2,2,6,6-tetramethyl-4-amino-piperidine-1-oxyl) was initially coupled with Boc-L-alanine, Boc-L-phenylalanine or Fmoc-L-aspartic acid beta-tert-butyl ester in the presence of BOP and DIPEA to afford the amino acid-conjugated nitroxides (Fig. 1A). After deprotection

using TFA (for the Boc- group) or piperidine (for the Fmoc- group), the resulting nitroxides

NACs 1-3 were subsequently linked with the trityl radical CT-03 to generate NATriPol-1,

NATriPol-2 and the precursor PAP-1 which was further treated with TFA to giveNATriPol-3.

These three NATriPols were purified by column chromatography on reversed-phase C18 and

thoroughly characterized by HRMS and EPR (See also SI, Figures S1, S2 and S16).

Room-temperature and low-temperature EPR studies of NATriPols 1-3

Fig. 2A and Fig. S2A show EPR spectra of NATriPols 1-3 in phosphate buffer at room

temperature. The spectra are very similar and asymmetric with two partially overlapping and

weak peaks at low field, one intense peak at medium field and one moderate peak at high field.

Our previous study showed that the separation between the low-field two peaks is inversely

proportional to the magnitude of the exchange interaction (J) in TN biradicals.[43] The almost

identical separations (4.0–4.6 G) between the two low-field peaks for NATriPol biradicals

indicate that they exhibit similar J values. EPR spectral simulations showed that both NATriPol-

1 and NATriPol-3 have similar mean J values with TEMTriPol-1 ($\sim$ 60 G, Table 1) which are

slightly larger than that of NATriPol-2 (48 G). These results indicate that the J values of

NATriPols and TEMTriPol-1 at room temperature are marginally affected by the substituents at

the α-position of amino acid linkers. Recent studies have shown that both the exchange and

dipolar interactions of biradicals are crucial for their DNP properties.[34, 37, 41, 44, 49] For this reason,

we recorded EPR spectra of NATriPols 1-3 in 6/4 (v/v) glycerol/H_2O glass-forming solutions at

low temperature ($\sim$ 220K) (Fig.2A and S2B).

A

NAC-1, R = CH₃
NAC-2, R = CH₂Ph
NAC-3, R= CH₂COOBuᵗ
NAC-4, R = CH₂S-trityl

NATriPol-1, R = CH₃
NATriPol-2, R = CH₂Ph
PAP-1, R = CH₂COOBuᵗ
NATriPol-3, R = CH₂COOH
PAP-2, R = CH₂S-trityl
NATriPol-4, R =CH₂S-SPy

B

Figure1. (A) Synthesis of NATriPols 1-4. (B) Synthesis of NATriPol-5 through efficient thiol-click reaction of NATriPol-4 with glutathione (GSH).
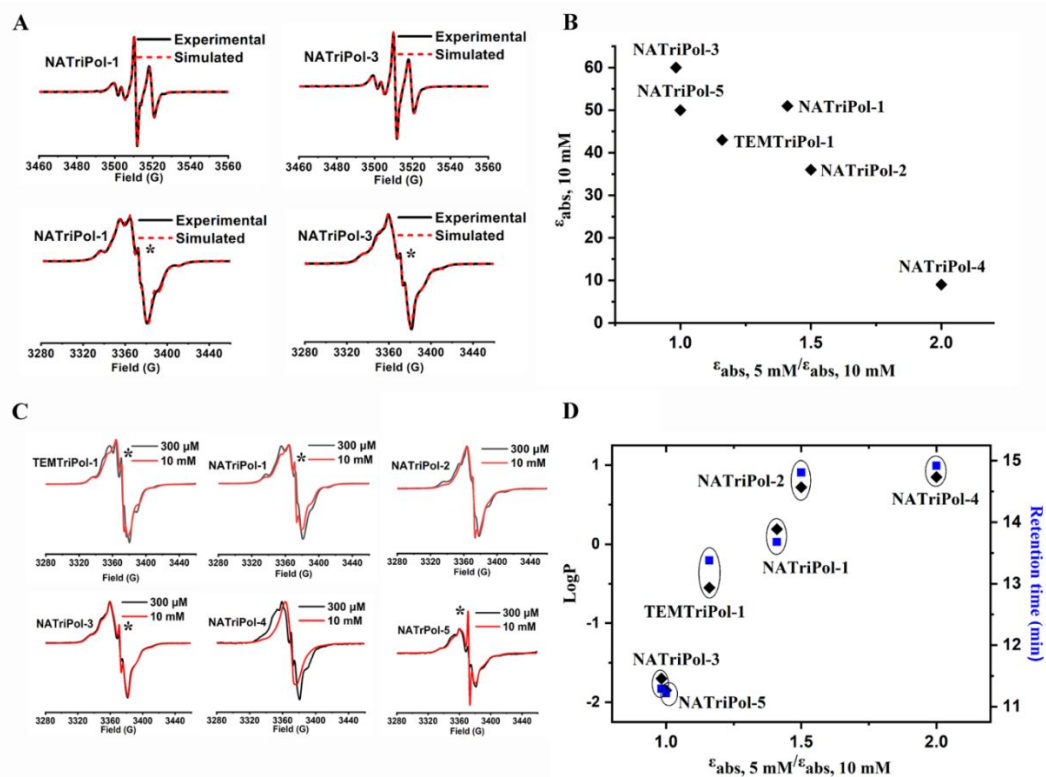
Figure 2. (A) Experimental (black solid line) and simulated (red dotted line) EPR spectra of 300 µM NATriPols in phosphate buffer (20 mM, pH 7.4) at room temperature (Top) or in glycerol/water (v/v, 60/40) at ~ 220 K (Bottom).(B) Comparison between experimentally determined DNP values ($\varepsilon_{abs,10mM}$ and the ratio $\varepsilon_{abs,5mM}/\varepsilon_{abs,10mM}$) for the NATriPols indicated. $\varepsilon_{abs,5mM}$ and $\varepsilon_{abs,10mM}$ represent the absolute DNP enhancements at biradical concentrations of 5 mM and 10 mM, respectively. (C) EPR spectra of 300 µM (black solid line) and 10 mM (red solid line) NATriPol 2-5 in glycerol/water (v/v, 60/40) at ~ 220K; EPR signals of each biradical at 300 µM and 10 mM were normalized. (D) Plots correlating octanol-water partition coefficient (LogP, black diamonds) and the retention times (RT, blue squares) with the ratio $\varepsilon_{abs,5mM}/\varepsilon_{abs,10mM}$. (A,C) "*" indicates signals from the trityl monoradical impurities whose fractions were determined by EPR simulation to be <1.3%, except for NATriPol-5 (2.5%) at 10 mM concentration.

Table 1. Exchange (J) and dipolar (D) interactions at ambient temperature (AT) and low temperature (LT), octanol−water partition coefficient (LogP), HPLC retention time (RT, min) and water solubility (WS, mM) of NATriPols and TEMTriPol-1 as well as experimental DNP parameters of NATriPols and other biradicals in the DNP juice (d_8-glycerol/D_2O/H_2O, 60/30/10, V/V/V) containing 0.25 M ^{13}C-^{15}N proline (unless indicated otherwise) at 18.8 T and 103 K.

Biradicals	J (AT)/G	J (LT)/G	D/G	LogP	RT	WS	$\varepsilon_{on/off}$	ε_{abs}	T_B	$\Sigma = \varepsilon_{abs}/\sqrt{(T_B/T_{off})}$
TEMTriPol-1	61	17	6	-0.55	13.4	75	50 (55)	43 (50)	3.7 (8)	198
NATriPol-1	64	18	6	0.19	13.7	174	60 (80)	51 (72)	3.5 (6)	244
NATriPol-2	48	17	5	0.72	14.8	101	40 (60)	36 (54)	7 (21)	122
NATriPol-3	64	18	6	-1.70	11.3	161	70 (65, 58[a])	60 (59, 48[a])	4.8 (8.5, 4[a])	243
NATriPol-4	64	18	6	0.85	14.9	N.D.	10 (20)	9 (18)	2 (4.7)	57
NATriPol-5	61	18	6	-1.85	11.2	190	56 (55, 43[a])	48 (50, 36[a])	4.5 (6, 2.2[a])	213
AMUPol							35[b]	19[c]	5[b]	76
AsymPolPOK[d]								24	5.8	

Experimental details and definition of $\varepsilon_{on/off}$, ε_{abs}, and T_B are given in the supporting information, together with CE ^1H DNP enhancement field profiles for the radicals TEMTriPol-1, NATriPol-1 and -5. The experimental parameters were obtained using 10 mM, 5 mM (in parenthesis) or [a] 15 mM biradical (in parenthesis). The same bleaching factor was calculated for NATriPol-1 and NATriPol-3 and the same value was applied to the other biradicals. Note that the bleaching effect could potentially be stronger for NATriPol-2 and NATriPol-4, due to their higher aggregation tendency (vide infra). The overall sensitivity gain Σ is calculated for a 10mM radical concentration. The mean values of J couplings were used in this study. [b] measured in this work under the same experimental conditions; [c]ε_{abs} was estimated based on the reported value of $\chi_{bleach} \cdot \chi_{depo}$ (0.54), see the reference[44]. [d] see the reference[34]. N.D. stands for "not detected".

It is evident that these biradicals are characterized by similar EPR spectra with almost identical overall separations (71 G) between the two outermost lines that are slightly larger than $2A_{ZZ}$ (~ 70 G), indicative of their similar but weak exchange interactions. Moreover, dipolar interactions that are averaged out at room temperature are now detectable, due to restricted molecular tumbling in the frozen state. Spectral simulation using our recently developed EPR program[43] showedthat NATriPols 1-3 and TEMTriPol-1 have almost the same dipolar (D = 5-6 G) and exchange (J = 17-19 G) interactions between the two spins (Table 1). The J values of

NATriPols in the frozen state are much smaller than those at room temperature possibly due to a change in the conformation equilibrium.[57] Collectively, these observations demonstrate that the α-position of amino acid linkers is a suitable choice for the structural modification site of TN biradicals whereby preserving the optimal electron-electron interactions.

Postmodification of 2-pyridine disulfide-appended NATriPol-4 with various thiols and EPR Studies

Having shown that the electron-electron interactions of TN biradicals remain nearly constant upon substitution at the α-position of the amino acid linkers, we subsequently aimed at synthesizing NATriPol-4 which contains a thiol-reactive 2-pyridyl disulfide at the α-position. As shown in Fig. 1A, the biradical precursor PAP-2 was obtained through two steps from 4-amino-TEMPO, N-Fmoc-S-trityl-L-cysteine and CT-03. NATriPol-4 was then obtained by TFA-induced deprotection of the thioether group in the presence of triethylsilane, followed by reaction with 2,2'-dithiodipyridine. Through a "click" reaction between 2-pyridyl disulfide moiety and thiols[58] new biradical polarizing agents can be readily prepared from NATriPol-4. Importantly, depending on the thiols used, these polarizing agents may exhibit tunable physicochemical properties but with the same electron-electron interactions. To prove this concept, we tested the reactivity of NATriPol-4 with various thiols including glutathione (GSH), cysteine (Cys) and 4-mercaptobenzoic acid (4-MBA) (Fig. 1B and Fig. S4). The thiol-click reaction was monitored by the formation of 2-mercaptopyridine which has a maximal UV-vis absorbance at 343 nm.[58] As shown in Fig. S4, the reaction of NATriPol-4 with 4-MBA was very fast and completed in less than 1 minute, while the reactions with Cys and GSH were completed in 4 and 5 minutes, respectively. The distinct reactivities between NATriPol-4 and thiols can be connected to

different pKa's of the thiols, with high reactivity for the thiol with low pKa. The highly efficient

formation of the disulfide conjugates was further confirmed by HPLC experiments (Fig. S4D).

To check if the linkage of the thiol groups affects the electron-electron interactions of the

disulfide conjugates, the room- and low-temperature EPR spectra of NATriPol-4 and NATriPol-

5 (the disulfide conjugate with GSH) were recorded and simulated (Fig. S2). Once again, both of

them have very similar J values of 56–64 G at room temperature and 16–18 G at ~ 220 K as well

as similar dipolar interactions of 5–6 G at ~ 220 K (Table 1). These values are fully consistent

with those from NATriPols 1-3 and TEMTriPol-1. Thus, we could conclude that the "click"

reaction of NATriPol-4 with thiols is an efficient postmodification approach to synthesize new

TN biradicals with tunable physicochemical properties.

Dynamic nuclear polarization studies on ^{13}C-^{15}N proline

The DNP performance of NATriPols in 3.2mm sapphire rotors was examined using a high-

field DNP setup (800 MHz/527 GHz). Firstly, ^{1}H-^{13}C cross polarization experiments were

carried out on frozen solutions of NATriPols in DNP juice (d_8-glycerol/D$_2$O/H$_2$O, 60/30/10,

V/V/V) containing 0.25 M ^{13}C-^{15}N proline at 103 K. The MAS frequency was set to 8 kHz

which was shown to be optimal for TN biradicals (e.g., TEMTriPol-1).[44] To assess the DNP

performance of the NATriPol biradical polarizing agents, we computed absolute signal gains

($\varepsilon_{abs} = \varepsilon_{on/off} \cdot \chi_{bleach} \cdot \chi_{depo}$), which take into account depolarization and bleaching effects, and the

sensitivity gain ($\Sigma = \varepsilon_{abs} / \sqrt{(T_B / T_{off})}$). The latter parameter represents the sensitivity gain

observed when performing DNP as compared to a MAS NMR experiment performed at the same

(cryogenic) temperature without DNP, as reported previously.[39, 59] At the 10 mM biradical

concentration, we observed paramagnetic bleaching factors (χ_{bleach}) of 0.85 for NATriPol-1 and

NATRiPol-3 (Table S8) in good agreement with reported values for TEMTriPol-1.[44] Similar to TEMTriPol-1, no depolarization was observed for these biradicals. When comparing absolute DNP enhancement factors (ε_{abs}) of NATriPols (Table 1), we observed strong variations with values ranging from 9 to 60 for ^{13}C-^{15}N proline at a 10 mM biradical concentration. The absolute signal gains of NATriPol-1 (ε_{abs} = 51), NATriPol-3 (ε_{abs} = 60) and NATriPol-5 (ε_{abs} = 48) were higher than the value found for TEMTriPol-1 (ε_{abs} = 43). It should be noted that under similar conditions, the ε_{abs} values of the widely used water-soluble AMUPol and the newly synthesized AsymPolPOK were reported to be 19 and 24[34], respectively.

Since both dipolar and exchange interactions are almost identical for the NATriPols under investigation, factors other than magnetic interactions are responsible for the strong variation in their experimentally observed DNP performance. Indeed, previous studies suggested that the formation of high local concentration zones of polarizing agents induced by inhomogeneous dispersion in the matrix is detrimental to their DNP properties.[29, 60] The aggregation of the trityl radical CT-03 which was used to synthesize NATriPols in this work was observed in glycerol/water mixture at low temperature.[61-62] Thus, it can be deduced that the self-aggregation of NATriPols driven by their hydrophobicity in the DNP matrix is mainly responsible for the difference in their DNP performances. Assuming that the self-aggregation occurs for NATriPols in the matrix, their DNP enhancements should increase when using lower radical concentrations. Hence, we measured absolute DNP enhancements of NATriPols at 5 mM biradical concentration ($\varepsilon_{abs, 5mM}$) and correlated the ratio of $\varepsilon_{abs, 5mM}/\varepsilon_{abs, 10mM}$ with the absolute enhancements observed at 10 mM concentration. As visible in Fig. 2B, the NATriPol variants that exhibit lower absolute enhancements at the 10 mM concentrations have significantly larger values of $\varepsilon_{abs, 5mM}/\varepsilon_{abs, 10mM}$, which we tentatively ascribe to their self-aggregation tendency.

Fig. 2B suggests that with the exception of NATriPol-1, the $\varepsilon_{abs,\ 10mM}$ values of the biradicals are inversely correlated with the ratios of $\varepsilon_{abs,\ 5mM}/\varepsilon_{abs,\ 10mM}$, indicating that the self-aggregation is a critical factor for the DNP efficiency of NATriPols. Note that, although NATriPol-1 exhibits a similar and moderate self-aggregation tendency as TEMTriPol-1, it shows a relatively higher $\varepsilon_{abs,\ 10mM}$ value than the latter. We attribute this effect to the relatively rigid linker of NATriPol-1 which leads to the improved and narrow distribution of the dipolar/exchange interactions. Generally, the distribution of the dipolar/exchange interactions originates from the flexibility of the linker which results in coexistence of many conformations in solution. As such, the biradical with a flexible linker has a broader distribution for its dipolar/exchange interactions compared to a compound with a rigid linker. Moreover, the interactions of the former exhibit a stronger dependence on temperature.[43, 57] Our variable-temperature EPR results showed that J values of TEMTriPol-1 increase by ~ 50% as compared to ~30% for NATriPol-1 as temperature increases from 300 K to 360 K (Figure S3 and Table S9). Moreover, the J distribution (ΔJ = 6.5 G, Table S1) of TEMTriPol-1 at room temperature is slightly larger than that of NATriPol-1 (6.0 G). These results consistently demonstrate that NATriPol-1 has a more rigid linker than TEMTriPol-1, accounting for the high DNP enhancement of the former.

To further verify the influence of self-aggregation of NATriPols, we recorded EPR spectra of NATriPols and TEMTriPol-1 at a high concentration (10 mM) and low temperature (~ 220K) in DNP buffer (Figure 2C). Interestingly, broad EPR single line signals were observed for NATriPol-4 and NATriPol-2 that exhibit the strongest self-aggregation tendency. Comparatively, NATriPol-1 and TEMTriPol-1 with moderate self-aggregation tendency exhibited narrower EPR lines. EPR spectral profiles of NATriPol-3 and NATriPol-5 with weak or no self-aggregation showed well resolved hyperfine splittings, similar to the corresponding

spectra obtained at 300 μM. We attribute the broad EPR single lines of NATriPol-4 and NATriPol-2 to significant exchange couplings among neighboring biradicals that result from self-aggregation and lead to a featureless EPR spectrum, as expected for multi-spin arrays where all spins are coupled.

Finally, we investigated factors that induce the self-aggregation of the NATriPols in aqueous solutions. For this purpose, we measured the octanol-water partition coefficients (LogP) and retention times (RTs) of NATriPols together with TEMTriPol-1 on a reversed-phase HPLC, both of which can be used to quantitatively describe the hydrophobicity of the biradicals. Again, the ratio $\varepsilon_{abs,\ 5mM}/\varepsilon_{abs,\ 10mM}$ seems to correlate with both LogP and RT, indicating that the hydrophobicity is mainly responsible for their self-aggregation (Fig. 2D). It is worth noting that the self-aggregation tendency of NATriPols and TEMTriPol-1 has no direct relationship with their water solubility. For example, the water solubility (174 mM, Table 1) of NATriPol-1 is much higher than that of TEMTriPol-1 (75 mM), although they have similar self-aggregation tendency. Indeed, the water solubility of NATriPol-1 is slightly higher than that of the hydrophilic NATriPol-3 (161 mM). Thus, good water solubility of polarizing agents, especially when the solubility is higher than the concentration used in DNP experiments, could not be the only indicator of their self-aggregation tendency in solutions.

Dynamic nuclear polarization studies on biomolecules

Since some of the newly synthesized NATriPols exhibit excellent DNP enhancements for ^{13}C-^{15}N proline due to their high hydrophilicity, we examined their potential for applications to complex biomolecules. First, we investigated whether the DNP enhancement seen for proline significantly differs for other amino acids. For this purpose, we tested the DNP performance of

the hydrophilic NATriPol-3 and NATriPol-5 on a $[^{13}C,^{15}N]$ labeled Algal amino-acid mixture containing 16 amino acids and compared our results to DNP experiments using AMUPol. In 1D ^{13}C CP MAS experiments (Table S10), we observed a DNP enhancement $\varepsilon_{on/off}$ = 48 for a sample prepared with 10 mM NATriPol-3. Notably, we measured a weaker enhancement ($\varepsilon_{on/off}$ = 35) for NATriPol-5, confirming the higher efficiency of NATriPol-3. Even though a decrease in enhancement ($\varepsilon_{on/off}$ = 48) is observed in comparison to standard proline ($\varepsilon_{on/off}$ = 70), the enhancements using NATriPol-3 were about 1.6-2 times higher than those seen for AMUPol ($\varepsilon_{on/off}$ = 30 for the labeled Algal mixture and $\varepsilon_{on/off}$ = 35 for proline, see Table S10). Moreover, considering the depolarization and bleaching effects, NATriPol-3 outperforms AMUPol by a factor 2.5 in terms of the absolute DNP enhancement[34, 44]. To probe amino-acid specific DNP enhancements, we conducted 2D proton-driven spin diffusion (PDSD) experiments with and without microwave irradiation using a 10 mM NATriPol-3 concentration (Fig. 3 and Fig. S6). These data allowed us to separate signal intensities of different types of amino acids including threonine, serine and aspartic acid (Fig. 3, left). When comparing 1D slices, we however only observed minor variations in the DNP performance of the different amino acids.
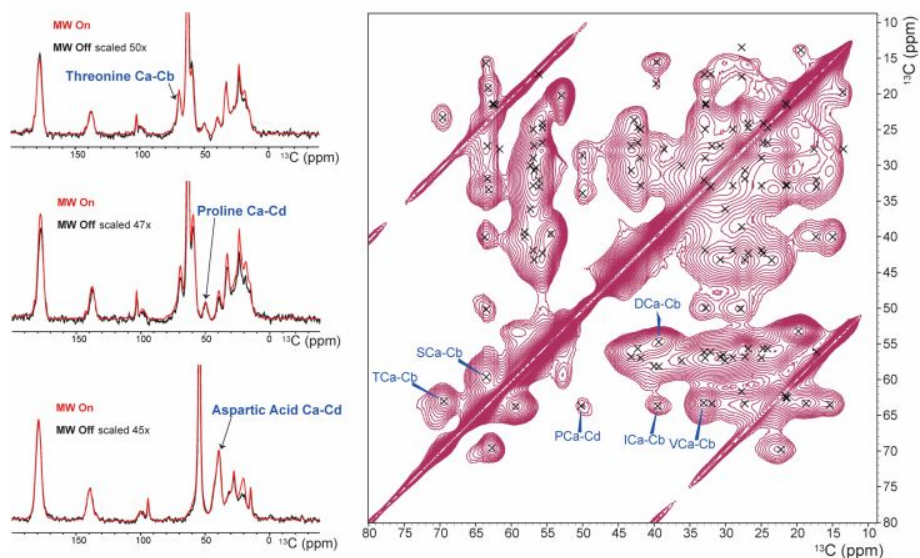
Figure 3. Right panel: aliphatic region of a 2D DNP-enhanced ^{13}C, ^{13}C PDSD spectrum of the Algal amino acid mixture in d_8-glycerol:D_2O:H_2O (60:30:10 v:v:v) and 10 mM NATriPol-3. Crosses represent chemical-shift predictions for the different amino acids, based on the respective BMRB average shift. The arrows (left) refer to 1D slices of isolated peaks (right) of specific amino acids that were used to calculate the relative enhancement factors.

The results shown in Fig. 3 suggest that our new NATriPol preparations can provide a significantly improved DNP enhancement compared to the current standard AMUPol. Therefore, we next examined their potential for applications to soluble proteins by testing their performance on ubiquitin, a regulatory protein that was already examined in DNP studies.[63] It is well known that enhancements measured on biomacromolecules are often reduced when compared to model substances,[5] possibly due to the complexity and internal dynamics of biological samples that affect their relaxation behavior. Unlike free amino-acid mixtures, proteins can exhibit local hydrophobic pockets that often engage in protein-protein or protein-lipid interactions. For example, the surface of ubiquitin contains a hydrophobic patch (comprising residues L8, I44, and V70) that form a prominent site of molecular recognition[64]. Thus, the biradicals may exhibit hydrophobic interactions with both the target protein and with other biradical molecules (i.e., self-aggregation). Both interactions are driven by the hydrophobicity of the biradicals and are detrimental to their DNP enhancements. To investigate any local interactions between NATriPols and ubiquitin we performed solution-state NMR titration experiments in which we added increasing amounts (0, 0.01 and 0.1 mM) of biradical into a 0.1 mM solution of [^{13}C,^{15}N] ubiquitin.

As a control, we prepared samples using TOTAPOL (Fig. S7). This allowed us to investigate potential local interactions between the protein and biradical, which could give rise to both chemical-shift perturbations as well as paramagnetic relaxation effects.[20] For all four cases,

we examined residue-specific chemical-shift perturbations (CSPs) and NMR signal intensities (Fig. S8-S11). In Fig. 4, zoom-ins of ^{15}N-HSQC spectra of ubiquitin are shown using TEMTriPol-1, ATriPol-5 and NATriPol-3 at increasing biradical concentrations. For TEMTriPol-1, we observed significant chemical-shift changes as well as reduced signal intensities (Fig. 4 & S9) that suggest a clear interaction between the biradical and the protein. Residues affected by the biradical included residues around Ile44 and Val70 that are part of the aforementioned hydrophobic patch of ubiquitin. These findings are in line with earlier results,[59, 65] indicating that the trityl radical CT-03 is prone to bind to proteins, driven by the hydrophobic interaction. For the more hydrophilic NATriPol-5, the CSPs were reduced but the signal intensity loss was still apparent for the mobile residues K48-Q49 and the C-terminal tail residue Arg72 when compared to pure ubiquitin (Fig. 4 and S10). Ultimately, the biradical NATriPol-3 left a large part of the spectrum unaffected, with no noticeable chemical shift changes (Fig. 4, right column), similar to results obtained using TOTAPOL (Fig. S8). Interestingly and unlike TOTAPOL, we still observed some signal loss in the case of NATriPol-3 for residues in the aforementioned protein regions which may be explained by the enhanced paramagnetic quenching of trityl vs. nitroxide radicals.[59]
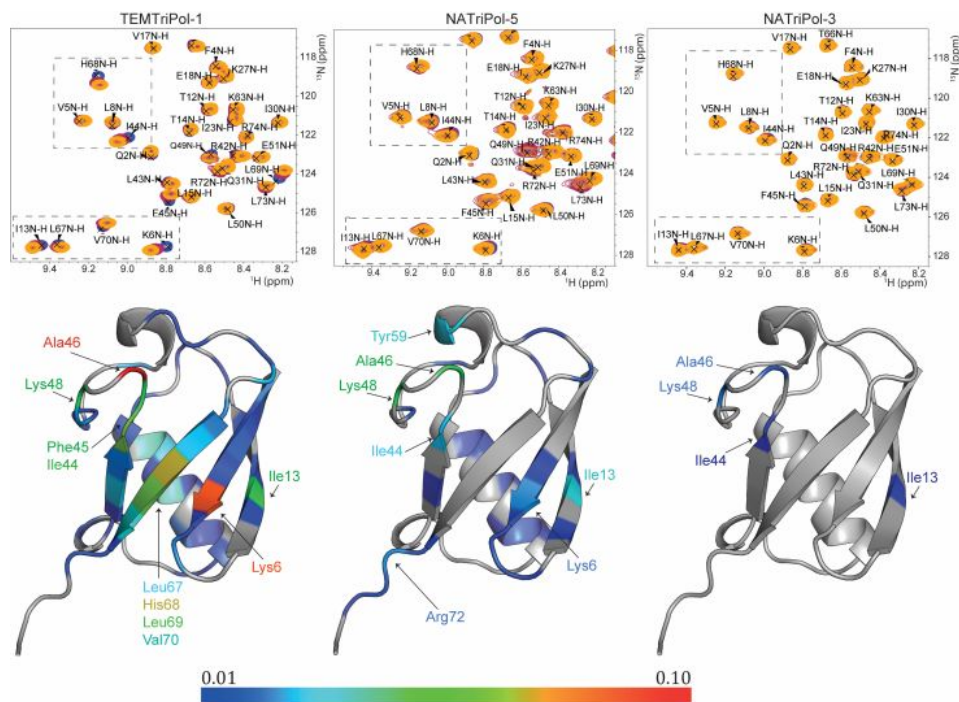
Figure 4. Upper panel: zoom-in on the ^{15}N-HSQC spectra of ubiquitin (0.1 mM, blue) in 90/10 H$_2$O/D$_2$O and after a titration with 0.01 mM (purple) and 0.1 mM (orange) biradical concentrations for TEMTriPol-1 (left), NATriPol-5 (middle) and NATriPol-3 (right). The regions exhibiting the biggest chemical shift perturbations (CSPs) are highlighted in dashed boxes. Lower panel: ubiquitin residues are highlighted which showed the strongest chemical-shift perturbations Δcs calculated using $\Delta cs = \sqrt{\delta_H^2 + (\delta_N/6.51)^2}$.
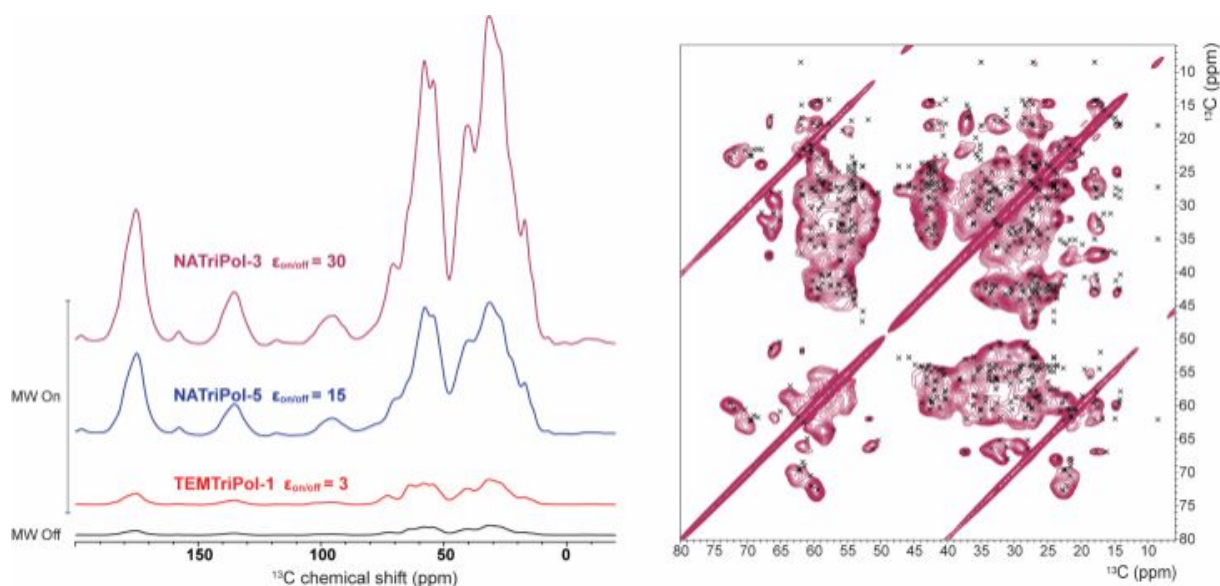
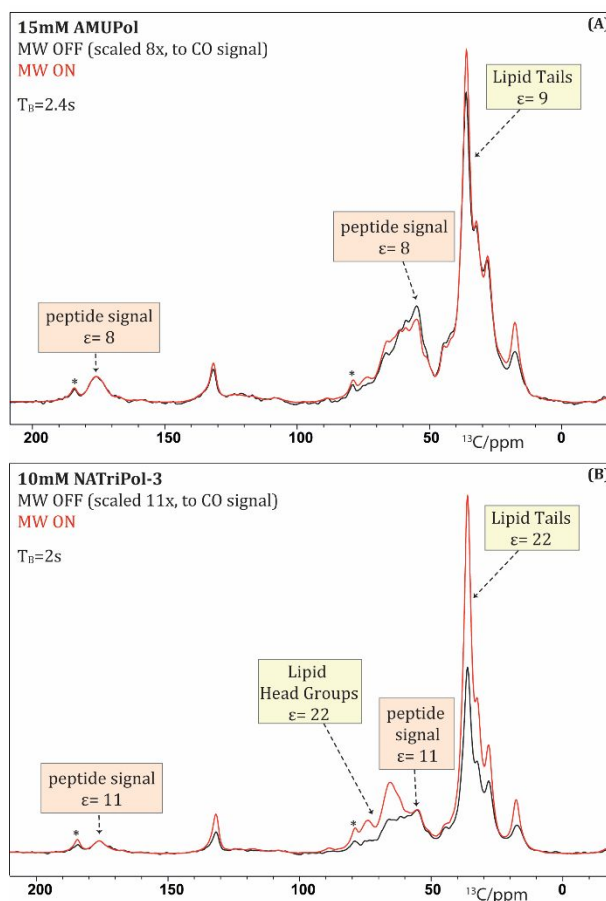**Figure 5.** Left: 1D DNP-enhanced ^{1}H-^{13}C CP spectra of ubiquitin (4 mM) in d$_8$-glycerol:D$_2$O:H$_2$O (60:30:10 v:v:v) and 10 mM biradical concentration. Three different biradicals were tested: TEMTriPol-1 (red), NATriPol-5 (in blue) and NATriPol-3 (purple). Right: the aliphatic region of the 2D ^{13}C, ^{13}C correlated PDSD experiment measuring ubiquitin with 10 mM NATriPol-3. Black crosses indicate NMR assignments (BMRB IDs 7111 & 15410).

Having established on an atomic level that NATriPol-3 and NATriPol-5 reveal reduced hydrophobic interactions with [^{13}C,^{15}N] ubiquitin in solution, in comparison to TEMTriPol-1, we conducted DNP experiments on both compounds. We compared our results to those of TEMTriPol-1 and AMUPol (see Table S10). Surprisingly, TEMTriPol-1 performs very poorly when measured on the ^{13}C-^{15}N labeled protein, with an enhancement ($\varepsilon_{on/off}$) of only 3 and a relatively short DNP build-up time (T_B = 800 ms) at a 10 mM biradical concentration (Fig. 5). The short DNP build-up time suggests close proximity between the biradical and the protein,[33] further confirming our NMR titration experiments. On the other hand, NATriPol-5 showed a superior DNP enhancement ($\varepsilon_{on/off}$ = 15, T_B = 1.6 s) for ubiquitin. The DNP signal increase achieved by NATriPol-3 was even higher, with an enhancement of 30 (T_B = 2.5s) (Fig. 5), which

is 10 times larger than TEMTriPol-1 and comparable to what we observed using AMUPol ($\varepsilon_{on/off}$ = 30, Table S10). Moreover, a two-dimensional PDSD spectrum (Fig. 5 right, and Fig. S12) confirmed our earlier observations[20, 24] that conducting ssNMR experiments at 800 MHz can improve spectral resolution compared to data obtained at 400 MHz[63] (see Fig. S13). In addition, the observed 2D correlation pattern was in good agreement with the NMR assignments (indicated black crosses in Fig. 5), indicating that our preparations contained properly folded ubiquitin. Taken together, both self-aggregation behavior and the tendency of TEMTriPol-1 to localize to hydrophobic protein residues contribute to its markedly low DNP efficiency. Both effects are reduced for the more hydrophilic NATriPol-3 and NATriPol-5, resulting in significantly higher DNP enhancements in a biomolecular context. Therefore, these findings suggest a direct relationship between hydrophilicity and DNP enhancement when using NATriPols for biological applications.

Finally, we tested our new biradical NATriPol-3 on the pore-forming membrane peptide Nisin[66]. DNP is particularly crucial for the study of membrane proteins and membrane embedded peptides (see the representative references[6, 10-11]).

Figure 6. (A): 1D DNP-enhanced ^{1}H-^{13}C CP spectra of the lipid II-bound state of ^{13}C labelled-nisin in DOPC liposomes, with 15 mM AMUPol. (B): 1D DNP-enhanced ^{1}H-^{13}C CP spectra of the lipid II-bound state of ^{13}C labelled-Nisin in DOPC liposomes, with 10 mM NATriPol-3. Yellow and orange boxes indicate NMR frequencies in which the observed signal is dominated by lipid and peptide contributions, respectively. (See Fig. S14 in the SI for corresponding 1D ^{13}C double-quantum spectra.)

As reported by Hong et al.[67], the structural and magnetic properties of the polarizing agents and their distribution in the membranes strongly influence the DNP enhancement in a lipid environment. To better rationalize the performance of our new biradicals, we determined the DNP enhancement for the ^{13}C signals of lipids and the (isotope-labeled) Nisin peptide alongside with the respective build-up times.

In Figure 6, we compare spectra of the lipid II-bound state of ^{13}C labelled-Nisin in DOPC liposomes prepared using published procedures[66] and employing a 15mM AMUPol concentration (Fig. 6A) as well as a 10mM NATriPol-3 concentration (Fig. 6B), respectively. In line with previous work[66], we found a moderate and uniform enhancement ($\varepsilon_{on/off,\ AMU} \approx 8$) using AMUPol. Instead, we observed a higher enhancement of the lipid signals ($\varepsilon_{on/off,\ NAT-3} \approx 22$), as well as for peptide signals ($\varepsilon_{on/off,\ NAT-3} \approx 11$) in the case of NATriPol-3. When taking into account the faster build-up time and the lower depolarisation factor, NATriPol-3 provides an improvement of a factor 2.4 on the peptide signal compared to AMUPol. The short build-up times measured in both samples suggest proper mixing of the polarizing agents in this system.

Remarkably, lipid signals are further enhanced in Figure 6B, which may be related to the slightly higher hydrophobicity of the TN biradical in comparison to the bisnitroxide, that favors interactions between the TN biradical and the lipid bilayer. Previous studies on nitroxide radicals in the presence of phospholipid membranes suggest that the physical location of the radical and especially the g-tensors alignment are critical factors for the DNP enhancement.[67] On one hand these studies demonstrate that introducing polarizing agents in the hydrophobic core of the lipid bilayer can diminish the enhancement gradient typically observed across the membrane.[68] On the other hand, the localisation of the radicals within the membrane can also be deleterious to the DNP enhancement.[69] Hence, a more systematic study of the performance of TN biradicals for the investigation of membrane proteins and polypeptides will be required in the future. However, the current results already suggest the beneficial use of the new class of biradicals together with the improved resolution achieved at high fields for ssNMR studies on complex biomolecules including membrane proteins.

Conclusions

In this work, we found that the α-position of the amino acid linkers in TN (aka TEMTriPols) biradicals is an ideal structural modification site since their dipolar and exchange interactions that are crucial for CE-DNP are marginally affected by the substituents at this position. Based on this result, we have developed an efficient post-modification strategy using the novel pyridine disulfide-containing NATriPol-4 to conveniently synthesize TN biradical-based polarizing agents with desirable physicochemical properties (e.g., high hydophilicity). Importantly, this universal postmodification strategy is also suitable for synthesis of other polarizing agents using the well established bioorthgonal reactions such as thiol-maleimide and yne-azide reactions. In addition, NATriPol-4 can also be covalently attached to the protein of interest or lipid by thiol-specific labelling, providing several potential advantages over exogenously added polarizing agents[68, 70-71].

Because of their favorable magnetic-field dependence, TN biradicals are ideal candidates for ultra high-field DNP studies but theirpractical application to biomolecules was thus far limited. We found that self-aggregation of TEMTriPol-1, so far the best TN biradical, and its hydrophobic interaction with biomolecules are the main reasons limiting its biomolecular applications, in spite of its good water solubility. Owing to the high hydrophilicity, the newly synthesized NATriPol-5 and NATriPol-3 exhibit 5- and 10-fold DNP improvements, respectively, compared to TEMTriPol-1 when applied to the globular protein ubiquitin. Excellent DNP performance of NATriPol-3 has been also confirmed by its application to a membrane peptide. Therefore, our present work represents the first step towards a better understanding of TN biradical-based polarizing agents and provides new routes for optimization of high-field polarizing agents for biomolecular applications. Considering that NATriPols still exhibit

hydrophobic interactions to a certain extent with proteins and membrane lipids, new polarizing agents based on the more hydrophilic trityl radicals such as TFO[72] and OX063[73] are expected to further enhance their biomolecular applications in future.

ASSOCIATED CONTENT

Supporting Information

Characterization of the compounds; EPR spectra and spectral simulation; quantification of enhancement, bleaching, and depolarization; thiol-disulfide exchange reactions of NATriPol-4; magnetic field-dependence of the Cross-effect ^{1}H DNP enhancement; 2D- ^{13}C,^{13}C PDSD and ^{15}N-HSQC spectra of a U[^{13}C,^{15}N] Algal mixture and U[^{13}C,^{15}N] ubiquitin; analysis of peak intensities and chemical shift perturbations (CSPs); comparison of 400 and 800 MHz DNP 2D PDSD spectra obtained on U[^{13}C,^{15}N] ubiquitin; 1D ^{13}C-DQSQ spectra of ^{13}C-Nisin in DOPC membranes.

AUTHOR INFORMATION

Corresponding Authors

Yangping Liu - Tianjin Key Laboratory on Technologies Enabling Development of Clinical Therapeutics and Diagnostics, School of Pharmacy, Tianjin Medical University, Tianjin 300070, P. R. China, E-mail: liuyangping@tmu.edu.cn

Marc Baldus- NMR Spectroscopy, Bijvoet Centre for Biomolecular Research, Utrecht University, 3584 CH Utrecht, The Netherlands; Email: m.baldus@uu.nl

Author Contributions

Y.P.L., M.B., W.X. Zhai and A.L.P. conceived and designed research. W.X. Zhai, X.Y.C., W.X. Zhang and Y.G.S. conducted the synthesis of NATriPols and their physicochemical characterization. A.R. and W.X. Zhai performed EPR spectral simulation. A.L.P., S.N., J.M.S. and M.W prepared the samples for the DNP measurements. A.L.P. performed the DNP experiments. All authors contributed to data analysis. Y.P.L., M.B., W.X. Zhai and A.L.P. cowrote the manuscript and all authors edited it.

‡These authors contributed equally.

Notes

There are no conflicts to declare.

REFERENCES

1. Ardenkjaer-Larsen, J. H.; Fridlund, B.; Gram, A.; Hansson, G.; Hansson, L.; Lerche, M. H.; Servin, R.; Thaning, M.; Golman, K., Increase in signal-to-noise ratio of > 10,000 times in liquid-state NMR. *Proc. Natl. Acad. Sci. U. S. A.* **2003,***100* (18), 10158-10163.

2. Lindale, J. R.; Eriksson, S. L.; Tanner, C. P. N.; Zhou, Z. J.; Colell, J. F. P.; Zhang, G. N.; Bae, J.; Chekmenev, E. Y.; Theis, T.; Warren, W. S., Unveiling coherently driven hyperpolarization dynamics in signal amplification by reversible exchange. *Nat. Commun.* **2019,***10*, 7.

3. Ni, Q. Z.; Daviso, E.; Can, T. V.; Markhasin, E.; Jawla, S. K.; Swager, T. M.; Temkin, R. J.; Herzfeld, J.; Griffin, R. G., High Frequency Dynamic Nuclear Polarization. *Acc. Chem. Res.* **2013,***46* (9), 1933-1941.

4. Rossini, A. J.; Zagdoun, A.; Lelli, M.; Lesage, A.; Coperet, C.; Emsley, L., Dynamic Nuclear Polarization Surface Enhanced NMR Spectroscopy. *Acc. Chem. Res.* **2013,***46* (9), 1942-1951.

5. Thankamony, A. S. L.; Wittmann, J. J.; Kaushik, M.; Corzilius, B., Dynamic nuclear polarization for sensitivity enhancement in modern solid-state NMR. *Prog. Nucl. Magn. Reson. Spectrosc.* **2017,***102*, 120-195.

6. Mak-Jurkauskas, M. L.; Bajaj, V. S.; Hornstein, M. K.; Belenky, M.; Griffin, R. G.; Herzfeld, J., Energy transformations early in the bacteriorhodopsin photocycle revealed by DNP-enhanced solid-state NMR. *Proc. Natl. Acad. Sci. U. S. A.* **2008,***105* (3), 883-888.

7. Koers, E. J.; Lopez-Deber, M. P.; Weingarth, M.; Nand, D.; Hickman, D. T.; Ndao, D. M.; Reis, P.; Granet, A.; Pfeifer, A.; Muhs, A., et al, Dynamic Nuclear Polarization NMR Spectroscopy: Revealing Multiple Conformations in Lipid-Anchored Peptide Vaccines. *Angew. Chem., Int. Ed.* **2013,***52* (41), 10905-10908.

8. Kaplan, M.; Cukkemane, A.; van Zundert, G. C. P.; Narasimhan, S.; Daniels, M.; Mance, D.; Waksman, G.; Bonvin, A.; Fronzes, R.; Folkers, G. E., et al, Probing a cell-embedded megadalton protein complex by DNP-supported solid-state NMR. *Nat. Methods* **2015,***12* (7), 649-652.

9. Ardenkjaer-Larsen, J. H.; Boebinger, G. S.; Comment, A.; Duckett, S.; Edison, A. S.; Engelke, F.; Griesinger, C.; Griffin, R. G.; Hilty, C.; Maeda, H., et al, Facing and Overcoming Sensitivity Challenges in Biomolecular NMR Spectroscopy. *Angew. Chem., Int. Ed.* **2015,***54* (32), 9162-9185.

10. Kaplan, M.; Narasimhan, S.; de Heus, C.; Mance, D.; van Doorn, S.; Houben, K.; Popov-Celeketic, D.; Damman, R.; Katrukha, E. A.; Jain, P., et al, EGFR Dynamics Change during Activation in Native Membranes as Revealed by NMR. *Cell* **2016,***167* (5), 1241-1251.

11. Joedicke, L.; Mao, J. F.; Kuenze, G.; Reinhart, C.; Kalavacherla, T.; Jonker, H. R. A.; Richter, C.; Schwalbe, H.; Meiler, J.; Preu, J., et al, The molecular basis of subtype selectivity of human kinin G-protein-coupled receptors. *Nat. Chem. Biol.* **2018,***14* (3), 284-290.

12. Zagdoun, A.; Casano, G.; Ouari, O.; Lapadula, G.; Rossini, A. J.; Lelli, M.; Baffert, M.; Gajan, D.; Veyre, L.; Maas, W. E., et al, A Slowly Relaxing Rigid Biradical for Efficient Dynamic Nuclear Polarization Surface-Enhanced NMR Spectroscopy: Expeditious Characterization of Functional Group Manipulation in Hybrid Materials. *J. Am. Chem. Soc.* **2012,***134* (4), 2284-2291.

13. Zagdoun, A.; Rossini, A. J.; Conley, M. P.; Gruning, W. R.; Schwarzwalder, M.; Lelli, M.; Franks, W. T.; Oschkinat, H.; Coperet, C.; Emsley, L., et al, Improved Dynamic Nuclear Polarization Surface-Enhanced NMR Spectroscopy through Controlled Incorporation of Deuterated Functional Groups. *Angew. Chem., Int. Ed.* **2013,***52* (4), 1222-1225.

14. Marker, K.; Pingret, M.; Mouesca, J. M.; Gasparutto, D.; Hediger, S.; De Paepe, G., A New Tool for NMR Crystallography: Complete C-13/N-15 Assignment of Organic Molecules at

Natural Isotopic Abundance Using DNP-Enhanced Solid-State NMR. *J. Am. Chem. Soc.* **2015,***137* (43), 13796-13799.

15. Kobayashi, T.; Perras, F. A.; Slowing, I. I.; Sadow, A. D.; Pruski, M., Dynamic Nuclear Polarization Solid-State NMR in Heterogeneous Catalysis Research. *ACS Catal.* **2015,***5* (12), 7055-7062.

16. Berruyer, P.; Lelli, M.; Conley, M. P.; Silverio, D. L.; Widdifield, C. M.; Siddiqi, G.; Gajan, D.; Lesage, A.; Copéret, C.; Emsley, L., Three-dimensional structure determination of surface sites. *J. Am. Chem. Soc.* **2017,***139* (2), 849-855.

17. Becerra, L. R.; Gerfen, G. J.; Temkin, R. J.; Singel, D. J.; Griffin, R. G., Dynamic nuclear polarization with a cyclotron resonance maser at 5 T. *Phys. Rev. Lett.* **1993,***71* (21), 3561-3564.

18. Becerra, L. R.; Gerfen, G. J.; Bellew, B. F.; Bryant, J. A.; Hall, D. A.; Inati, S. J.; Weber, R. T.; S., U. N.; Prisner, T. F.; Mcdermott, A. E., A Spectrometer for Dynamic Nuclear Polarization and Electron Paramagnetic Resonance at High Frequencies. *J. Magn. Reson.* **1995,***117* (1), 28-40.

19. Matsuki, Y.; Takahashi, H.; Ueda, K.; Idehara, T.; Ogawa, I.; Toda, M.; Akutsu, H.; Fujiwara, T., Dynamic nuclear polarization experiments at 14.1 T for solid-state NMR. *Phys. Chem. Chem. Phys.* **2010,***12* (22), 5799-5803.

20. Koers, E. J.; van der Cruijsen, E. A. W.; Rosay, M.; Weingarth, M.; Prokofyev, A.; Sauvee, C.; Ouari, O.; van der Zwan, J.; Pongs, O.; Tordo, P., et al, NMR-based structural biology enhanced by dynamic nuclear polarization at high magnetic field. *J. Biomol. NMR* **2014,***60* (2-3), 157-168.

21. Bjorgvinsdottir, S.; Walder, B. J.; Pinon, A. C.; Yarava, J. R.; Emsley, L., DNP enhanced NMR with flip-back recovery. *J. Magn. Reson.* **2018,***288*, 69-75.

22. Wisser, D.; Karthikeyan, G.; Lund, A.; Casano, G.; Karoui, H.; Yulikov, M.; Menzildjian, G.; Pinon, A. C.; Purea, A.; Engelke, F., et al, BDPA-Nitroxide Biradicals Tailored for Efficient Dynamic Nuclear Polarization Enhanced Solid-State NMR at Magnetic Fields up to 21.1 T. *J. Am. Chem. Soc.* **2018,***140* (41), 13340-13349.

23. Lund, A.; Casano, G.; Menzildjian, G.; Kaushik, M.; Stevanato, G.; Yulikov, M.; Jabbour, R.; Wisser, D.; Renom-Carrasco, M.; Thieuleux, C., et al, TinyPols: a family of water-soluble binitroxides tailored for dynamic nuclear polarization enhanced NMR spectroscopy at 18.8 and 21.1 T. *Chem. Sci.* **2020,***11* (10), 2810-2818.

24. Fricke, P.; Mance, D.; Chevelkov, V.; Giller, K.; Becker, S.; Baldus, M.; Lange, A., High resolution observed in 800 MHz DNP spectra of extremely rigid type III secretion needles. *J. Biomol. NMR* **2016,***65* (3-4), 121-126.

25. Hu, K. N.; Yu, H. H.; Swager, T. M.; Griffin, R. G., Dynamic nuclear polarization with biradicals. *J. Am. Chem. Soc.* **2004,***126* (35), 10844-10845.

26. Matsuki, Y.; Maly, T.; Ouari, O.; Karoui, H.; Le Moigne, F.; Rizzato, E.; Lyubenova, S.; Herzfeld, J.; Prisner, T.; Tordo, P., et al, Dynamic Nuclear Polarization with a Rigid Biradical. *Angew. Chem., Int. Ed.* **2009,***48* (27), 4996-5000.

27. Kiesewetter, M. K.; Corzilius, B.; Smith, A. A.; Griffin, R. G.; Swager, T. M., Dynamic Nuclear Polarization with a Water-Soluble Rigid Biradical. *J. Am. Chem. Soc.* **2012,***134* (10), 4537-4540.

28. Sauvee, C.; Rosay, M.; Casano, G.; Aussenac, F.; Weber, R. T.; Ouari, O.; Tordo, P., Highly Efficient, Water-Soluble Polarizing Agents for Dynamic Nuclear Polarization at High Frequency. *Angew. Chem., Int. Ed.* **2013,***52* (41), 10858-10861.

The Journal of Physical Chemistry

29. Zagdoun, A.; Casano, G.; Ouari, O.; Schwarzwalder, M.; Rossini, A. J.; Aussenac, F.; Yulikov, M.; Jeschke, G.; Coperet, C.; Lesage, A., et al, Large Molecular Weight Nitroxide Biradicals Providing Efficient Dynamic Nuclear Polarization at Temperatures up to 200 K. *J. Am. Chem. Soc.* **2013,***135* (34), 12790-12797.

30. Kubicki, D. J.; Casano, G.; Schwarzwalder, M.; Abel, S.; Sauvee, C.; Ganesan, K.; Yulikov, M.; Rossini, A. J.; Jeschke, G.; Coperet, C.; Lesage, A., et al, Rational design of dinitroxide biradicals for efficient cross-effect dynamic nuclear polarization. *Chem. Sci.* **2016,***7* (1), 550-558.

31. Jagtap, A. P.; Geiger, M. A.; Stoppler, D.; Orwick-Rydmark, M.; Oschkinat, H.; Sigurdsson, S. T., bcTol: a highly water-soluble biradical for efficient dynamic nuclear polarization of biomolecules. *Chem. Commun.* **2016,***52* (43), 7020-7023.

32. Thurber, K. R.; Tycko, R., Theory for cross effect dynamic nuclear polarization under magic-angle spinning in solid state nuclear magnetic resonance: The importance of level crossings. *J. Chem. Phys.* **2012,***137* (8), 084508.

33. Mance, D.; Gast, P.; Huber, M.; Baldus, M.; Ivanov, K. L., The magnetic field dependence of cross-effect dynamic nuclear polarization under magic angle spinning. *J. Chem. Phys.* **2015,***142* (23), 234201.

34. Mentink-Vigier, F.; Marin-Montesinos, I.; Jagtap, A. P.; Halbritter, T.; van Tol, J.; Hediger, S.; Lee, D.; Sigurdsson, S. T.; De Paepe, G., Computationally Assisted Design of Polarizing Agents for Dynamic Nuclear Polarization Enhanced NMR: The AsymPol Family. *J. Am. Chem. Soc.* **2018,***140* (35), 11013-11019.

35. Mentink-Vigier, F.; Barra, A. L.; van Tol, J.; Hediger, S.; Lee, D.; De Paepe, G., De novo prediction of cross-effect efficiency for magic angle spinning dynamic nuclear polarization. *Phys. Chem. Chem. Phys.* **2019,***21* (4), 2166-2176.

36. Equbal, A.; Leavesley, A.; Jain, S. K.; Han, S. I., Cross-Effect Dynamic Nuclear Polarization Explained: Polarization, Depolarization, and Oversaturation. *J. Phys. Chem. Lett.* **2019,***10* (3), 548-558.

37. Mathies, G.; Caporini, M. A.; Michaelis, V. K.; Liu, Y. P.; Hu, K. N.; Mance, D.; Zweier, J. L.; Rosay, M.; Baldus, M.; Griffin, R. G., Efficient Dynamic Nuclear Polarization at 800 MHz/527 GHz with Trityl-Nitroxide Biradicals. *Angew. Chem., Int. Ed.* **2015,***54* (40), 11770-11774.

38. Takahashi, H.; Fernandez-De-Alba, C.; Lee, D.; Maurel, V.; Gambarelli, S.; Bardet, M.; Hediger, S.; Barra, A. L.; De Paepe, G., Optimization of an absolute sensitivity in a glassy matrix during DNP-enhanced multidimensional solid-state NMR experiments. *J. Magn. Reson.* **2014,***239*, 91-99.

39. Mentink-Vigier, F.; Paul, S.; Lee, D.; Feintuch, A.; Hediger, S.; Vega, S.; De Paepe, G., Nuclear depolarization and absolute sensitivity in magic-angle spinning cross effect dynamic nuclear polarization. *Phys. Chem. Chem. Phys.* **2015,***17* (34), 21824-21836.

40. Perras, F. A.; Sadow, A.; Pruski, M., In Silico Design of DNP Polarizing Agents: Can Current Dinitroxides Be Improved? *ChemPhysChem* **2017,***18* (16), 2279-2287.

41. Gast, P.; Mance, D.; Zurlo, E.; Ivanov, K. L.; Baldus, M.; Huber, M., A tailored multi-frequency EPR approach to accurately determine the magnetic resonance parameters of dynamic nuclear polarization agents: application to AMUPol. *Phys. Chem. Chem. Phys.* **2017,***19* (5), 3777-3781.

37

42. Liu, Y. P.; Villamena, F. A.; Rockenbauer, A.; Zweier, J. L., Trityl-nitroxide biradicals as unique molecular probes for the simultaneous measurement of redox status and oxygenation. *Chem. Commun.* **2010,** *46* (4), 628-630.

43. Liu, Y. P.; Villamena, F. A.; Rockenbauer, A.; Song, Y. G.; Zweier, J. L., Structural Factors Controlling the Spin-Spin Exchange Coupling: EPR Spectroscopic Studies of Highly Asymmetric Trityl-Nitroxide Biradicals. *J. Am. Chem. Soc.* **2013,** *135* (6), 2350-2356.

44. Mentink-Vigier, F.; Mathies, G.; Liu, Y. P.; Barra, A. L.; Caporini, M. A.; Lee, D.; Hediger, S.; Griffin, R. G.; De Paepe, G., Efficient cross-effect dynamic nuclear polarization without depolarization in high-resolution MAS NMR. *Chem. Sci.* **2017,** *8* (12), 8150-8163.

45. Hu, K. N.; Bajaj, V. S.; Melanie, R.; Griffin, R. G., High-frequency dynamic nuclear polarization using mixtures of TEMPO and trityl radicals. *J. Chem. Phys.* **2007,** *126* (4), 10844.

46. Dane, E. L.; Maly, T.; Debelouchina, G. T.; Griffin, R. G.; Swager, T. M., Synthesis of a BDPA-TEMPO Biradical. *Org. Lett.* **2009,** *11* (9), 1871-1874.

47. Pinto, L. F.; Marin-Montesinos, I.; Lloveras, V.; Munoz-Gomez, J. L.; Pons, M.; Veciana, J.; Vidal-Gancedo, J., NMR signal enhancement of > 50 000 times in fast dissolution dynamic nuclear polarization. *Chem. Commun.* **2017,** *53* (26), 3757-3760.

48. Munoz-Gomez, J. L.; Marin-Montesinos, I.; Lloveras, V.; Pons, M.; Vidal-Gancedo, J.; Veciana, J., Novel PTM-TEMPO Biradical for Fast Dissolution Dynamic Nuclear Polarization. *Org. Lett.* **2014,** *16* (20), 5402-5405.

49. Zhai, W. X.; Feng, Y. L.; Liu, H. Q.; Rockenbauer, A.; Mance, D.; Li, S. Y.; Song, Y. G.; Baldus, M.; Liu, Y. P., Diastereoisomers of L-proline-linked trityl-nitroxide biradicals: synthesis and effect of chiral configurations on exchange interactions. *Chem. Sci.* **2018,** *9* (19), 4381-4391.

50. Equbal, A.; Tagami, K.; Han, S., Balancing dipolar and exchange coupling in biradicals to maximize cross effect dynamic nuclear polarization. *Phys. Chem. Chem. Phys.* **2020,** *22* (24), 13569-13579.

51. Sauvee, C.; Casano, G.; Abel, S.; Rockenbauer, A.; Akhmetzyanov, D.; Karoui, H.; Siri, D.; Aussenac, F.; Maas, W.; Weber, R. T., et al, Tailoring of Polarizing Agents in the bTurea Series for Cross-Effect Dynamic Nuclear Polarization in Aqueous Media. *Chem.-Eur. J.* **2016,** *22* (16), 5598-5606.

52. Song, C.; Hu, K. N.; Joo, C. G.; Swager, T. M.; Griffin, R. G., TOTAPOL: a biradical polarizing agent for dynamic nuclear polarization experiments in aqueous media. *J. Am. Chem. Soc.* **2006,** *128* (35), 11385-11390.

53. Liu, Y. P.; Villamena, F. A.; Sun, J.; Xu, Y.; Dhimitruka, I.; Zweier, J. L., Synthesis and characterization of ester-derivatized tetrathiatriarylmethyl radicals as intracellular oxygen probes. *J. Org. Chem.* **2008,** *73* (4), 1490-1497.

54. Rockenbauer, A.; Korecz, L., Automatic computer simulations of ESR spectra. *Appl. Magn. Reson.* **1996,** *10* (1-3), 29-43.

55. Bodenhausen, G.; Ruben, D. J., Natural abundance nitrogen-15 NMR by enhanced heteronuclear spectroscopy *Chem. Phys. Lett.* **1980,** *69*, 185-189.

56. Fung, B. M.; Khitrin, A. K.; Ermolaev, K., An improved broadband decoupling sequence for liquid crystals and solids. *J. Magn. Reson.* **2000,** *142* (1), 97-101.

57. Tagami, K.; Equbal, A.; Kaminker, I.; Kirtman, B.; Han, S. I., Biradical rotamer states tune electron J coupling and MAS dynamic nuclear polarization enhancement. *Solid State Nucl. Magn. Reson.* **2019,** *101*, 12-20.

58. Grassetti, D. R.; Jr, J. F. M., Determination of sulfhydryl groups with 2,2′ - or 4,4′ - dithiodipyridine. *Arch. Biochem. Biophys.* **1967,***119* (1), 41-49.

59. Corzilius, B.; Andreas, L. B.; Smith, A. A.; Ni, Q. Z.; Griffin, R. G., Paramagnet induced signal quenching in MAS-DNP experiments in frozen homogeneous solutions. *J. Magn. Reson.* **2014,***240*, 113-123.

60. Barnes, A. B.; De Paepe, G.; van der Wel, P. C. A.; Hu, K. N.; Joo, C. G.; Bajaj, V. S.; Mak-Jurkauskas, M. L.; Sirigiri, J. R.; Herzfeld, J.; Temkin, R. J., et al, High-field dynamic nuclear polarization for solid and solution biological NMR. *Appl. Magn. Reson.* **2008,***34* (3-4), 237-263.

61. Marin-Montesinos, I.; Paniagua, J. C.; Vilaseca, M.; Urtizberea, A.; Luis, F.; Feliz, M.; Lin, F.; Van Doorslaer, S.; Pons, M., Self-assembled trityl radical capsules - implications for dynamic nuclear polarization. *Phys. Chem. Chem. Phys.* **2015,***17* (8), 5785-5794.

62. Marin-Montesinos, I.; Paniagua, J. C.; Peman, A.; Vilaseca, M.; Luis, F.; Van Doorslaer, S.; Pons, M., Paramagnetic spherical nanoparticles by the self-assembly of persistent trityl radicals. *Phys. Chem. Chem. Phys.* **2016,***18* (4), 3151-3158.

63. Narasimhan, S.; Scherpe, S.; Paioni, A. L.; van der Zwan, J.; Folkers, G. E.; Ovaa, H.; Baldus, M., DNP-Supported Solid-State NMR Spectroscopy of Proteins Inside Mammalian Cells. *Angew. Chem., Int. Ed.* **2019,***58*, 12969-12973.

64. Singh, R. K.; Kazansky, Y.; Wathieu, D.; Fushman, D., Hydrophobic Patch of Ubiquitin is Important for its Optimal Activation by Ubiquitin Activating Enzyme E1. *Anal. Chem.* **2017,***89* (15), 7852-7860.

65. Song, Y. G.; Liu, Y. P.; Liu, W. B.; Villamena, F. A.; Zweier, J. L., Characterization of the binding of the Finland trityl radical with bovine serum albumin. *RSC Adv.* **2014,***4* (88), 47649-47656.

66. Medeiros-Silva, J.; Jekhmane, S.; Paioni, A. L.; Gawarecka, K.; Baldus, M.; Swiezewska, E.; Breukink, E.; Weingarth, M., High-resolution NMR studies of antibiotics in cellular membranes. *Nat. Commun.* **2018,***9*, 10.

67. Liao, S. Y.; Lee, M.; Wang, T.; Sergeyev, I. V.; Hong, M., Efficient DNP NMR of membrane proteins: sample preparation protocols, sensitivity, and radical location. *J. Biomol. NMR* **2016,***64* (3), 223-237.

68. Smith, A. N.; Caporini, M. A.; Fanucci, G. E.; Long, J. R., A Method for Dynamic Nuclear Polarization Enhancement of Membrane Proteins. *Angew. Chem., Int. Ed.* **2015,***54* (5), 1542-1546.

69. Salnikov, E. S.; Sarrouj, H.; Reiter, C.; Aisenbrey, C.; Purea, A.; Aussenac, F.; Ouari, O.; Tordo, P.; Fedotenko, I.; Engelke, F., et al, Solid-State NMR/Dynamic Nuclear Polarization of Polypeptides in Planar Supported Lipid Bilayers. *J. Phys. Chem. B* **2015,***119* (46), 14574-14583.

70. Armstrong, B. D.; Jennifer, C.; Carlos, L.; Wesener, D. A.; Wayne, H.; Silvia, C.; Songi, H., Site-specific hydration dynamics in the nonpolar core of a molten globule by dynamic nuclear polarization of water. *J. Am. Chem. Soc.* **2011,***133* (15), 5987.

71. van der Cruijsen, E. A. W.; Koers, E. J.; Sauvée, C.; Hulse, R. E.; Weingarth, M.; Ouari, O.; Perozo, E.; Tordo, P.; Baldus, M., Biomolecular DNP-Supported NMR Spectroscopy using Site-Directed Spin Labeling. *Chem.-Eur. J.* **2015,***21* (37), 12971-12977.

72. Qu, Y. Y.; Li, Y. C.; Tan, X. L.; Zhai, W. X.; Han, G. F.; Hou, J. L.; Liu, G. Q.; Song, Y. G.; Liu, Y. P., Synthesis and Characterization of Hydrophilic Trityl Radical TFO for Biomedical and Biophysical Applications. *Chem.-Eur. J.* **2019,***25* (33), 7888-7895.

1
2
3
4
5
6
7
8
9
10
11
12
13
14
15
16
17
18
19
20
21
22
23
24
25
26
27
28
29
30
31
32
33
34
35
36
37
38
39
40
41
42
43
44
45
46
47
48
49
50
51
52
53
54
55
56
57
58
59
60

73. Ardenkjaer-Larsen, J. H.; Laursen, I.; Leunbach, I.; Ehnholm, G.; Wistrand, L. G.; Petersson, J. S.; Golman, K., EPR and DNP properties of certain novel single electron contrast agents intended for oximetric imaging. *J. Magn. Reson.* **1998,***133* (1), 1-12.

1
2
3
4
5
6
7
8
9
10
11
12
13
14
15
16
17
18
19
20
21
22
23
24
25
26
27
28
29
30
31
32
33
34
35
36
37
38
39
40
41
42
43
44
45
46
47
48
49
50
51
52
53
54
55
56
57
58
59
60

TOC Graphic